



	Prediction of the bed expansion of a liquid fluidized bed bioreactor applied to wastewater treatment and biogas production
	Victor Oliveira Ferreira, Daniel Silva Junior, Karla Raphaela Braga de Melo, Bruno Blais, & Gabriela Cantarelli Lopes
Date:	2023
Type:	Article de revue / Article
Référence: Citation:	Ferreira, V. O., Silva Junior, D., de Melo, K. R. B., Blais, B., & Lopes, G. C. (2023). Prediction of the bed expansion of a liquid fluidized bed bioreactor applied to wastewater treatment and biogas production. Energy Conversion and Management, 290, 117224 (10 pages). https://doi.org/10.1016/j.enconman.2023.117224

Document en libre accès dans PolyPublie Open Access document in PolyPublie

URL de PolyPublie: PolyPublie URL:	https://publications.polymtl.ca/53780/	
Version:	Version finale avant publication / Accepted version Révisé par les pairs / Refereed	
Conditions d'utilisation: Terms of Use:	Creative Commons Attribution-Utilisation non commerciale-Pas d'oeuvre dérivée 4.0 International / Creative Commons Attribution- NonCommercial-NoDerivatives 4.0 International (CC BY-NC-ND)	

Document publié chez l'éditeur officiel Document issued by the official publisher

Titre de la revue: Journal Title:	Energy Conversion and Management (vol. 290)		
Maison d'édition: Publisher:	Elsevier		
URL officiel: Official URL:	https://doi.org/10.1016/j.enconman.2023.117224		
Mention légale: Legal notice:			

Prediction of the bed expansion of a liquid fluidized bed bioreactor applied to wastewater treatment and biogas production

Victor Oliveira Ferreira ^b, Daniel Silva Junior ^a, Karla R. B. Melo ^b, Bruno Blais ^c,

Gabriela C. Lopes ^{a,b*}

- ^a Department of Chemical Engineering, Federal University of São Carlos, Rod.
 Washington Luiz, km 235 SP 310, São Carlos SP, 13565-905, Brazil
- b Chemical Engineering Graduate Program, Federal University of São Carlos, Rod.
 Washington Luiz, km 235 SP 310, São Carlos SP, 13565-905, Brazil
- c Research Unit for Industrial Flows Processes (URPEI), Department of Chemical Engineering, École Polytechique de Montréal, PO Box 6079, Stn Centre-Ville, Montréal, QC, Canada, H3C 3A7
 - * Corresponding author. Tel: +55 16 3351-8920. E-mail address: gclopes@ufscar.br

ABSTRACT

5

10

15

20

25

The high potential of water treatment and biogas production systems using liquid fluidization is still underexplored. The design of this equipment is usually done using the simple Richardson-Zaki equation for bed expansion predictions, which is powerful but overlooks the interactions between fluid and particles. In this work, an alternative method based on a force balance on the bed and drag correlations to estimate the bed porosity was proposed. The accuracy of the methods was assessed by comparing bed porosity estimations with experiments carried out in a wide range of regimes (Reynolds numbers between 498 and 18664), using 7 different particles with varied diameters (2.66 to 6.37 mm) and densities (1022 to 3585 kg/m³). On average, the fitting between the Richardson-Zaki equation and the experimental results was improved by 60% when the wall effects were considered. The alternative approach using the drag correlations showed promising results, presenting a coefficient of determination higher

than 80% for all particles, and better precision in 4 out of the 7 particles compared to Richardson-Zaki. The results show that, in general, both the Richardson-Zaki equation and the drag correlation approach can be used to predict the liquid fluidized bed expansion. However, the proposed approach using drag correlations showed more reliable results, especially when the Rong drag model was applied, with an average coefficient of determination of 0.92. Comparisons with other results in the literature confirm the extent and the scalability of the method. The use of the proposed method to estimate the liquid fluidized bed expansion allows for easier and safer applicability of the technology in areas such as wastewater treatment and biogas production.

KEYWORDS

30

35

40

45

50

Liquid-Solids Fluidization, Biogas, Wastewater Treatment, Richardson-Zaki equation, Drag Correlations, Bed Expansion.

1. INTRODUCTION

Liquid-solid fluidized beds (LSFB) are applied in many processes such as drinking water production [1], crystallization [2], particles classification [3], heat transfer [4], advanced oxidation processes [5], bioartificial devices [6], wastewater treatment with biogas and others [7]. In this type of equipment, the solids are lifted by the uprising liquid injected at velocities between the minimum fluidization and the terminal velocity of the particles. Consequently, the particles are held up in a uniformly dispersed, contact-driven dynamic. Among the main advantages of LSFBs compared to fixed beds is that the porosity of the bed can be easily increased by incrementing the inlet flow rate at a constant pressure drop [8], making the operation conditions more manageable.

Wastewater treatment with biogas production using LSFB bioreactors is particularly popular due to its versatility, low cost of maintenance [5], self-sustainability, and low

environmental impact in comparison with traditional techniques using inorganic reactants (usually strong bases or strong acids). The process consists of fluidizing particles carrying bioactive material, which consumes the organic matter present in the influent. It produces well-treated non-aggressive effluent and biogases (*e.g.*, methane and hydrogen) [9]. In such process, the composition of the products can be controlled by varying the microorganism and the influents. Additionally, the effectiveness of the influent conversion is sensitive to the carrier particle, which can be made of different polymers and ceramics [10].

According to Fraia *et al.* [11], wastewater treatment plants can be highly energy-consuming industries. However, the LSFB anaerobic bioreactors can decrease external energy consumption since the biogas product from the bioreactions can be used as fuel for energy generators, making the process cheap and self-sustainable [12]. The fluidization can help in the process because it increases the mass transfer between the fresh influent and the bioactive particles compared to slurry or fixed bed bioreactors.

Significant constraints regarding the LSFB bioreactors are related to the limited understanding of their fluid dynamics, leading to operational issues [12] and design limitations [13]. Most of the designs rely upon empirical equations based on experiments with hard, heavy particles. Among the design equations, the Richardson-Zaki equation (R-Z) [14] is particularly popular due to its simplicity and precision in predicting the LSFBs expansion. This equation (in its extended version) is

70

55

60

65

$$\frac{U}{U_{t,\infty}} = k\varepsilon^n \tag{1}$$

where U is the superficial velocity of the fluid, $U_{t,\infty}$ the terminal settling velocity of the particles $(U_{t,\infty} = Re_{t,\infty}\mu/d_p\rho)$, where μ and ρ are the dynamic viscosity and density of the fluid, respectively), and ε the fluid fraction inside the bed region, also referred to as bed voidage or

porosity. In Equation (1, k and n are empirical parameters. The parameter n is related to the characteristics of the flow, varying between 4.60 and 4.90 for particles in the Stokes regime $(Re_{t,\infty} < 0.2, Ar < 4)$ and 2.39 - 2.40 in the Newton regime $(Re_{t,\infty} > 500, Ar > 85000)$. For the region between the Stokes and Newton regimes, the correlation proposed by Khan & Richardson [15] (Equation (2) can be used to calculate n as a function of the Archimedes number $(Ar = gd_p^3 \rho(\rho_p - \rho)/\mu^2)$.

$$\frac{4.8 - n}{n - 2.4} = 0.043Ar^{0.57} \tag{2}$$

There are other accurate correlations in the literature to determine n, such as the ones proposed by Wallis [16], Garside & Al-Dibouni [17], and Rowe [18]. Notwithstanding, Equation (2 is significantly more convenient since it does not depend on experimental efforts or other correlations to determine the terminal Reynolds of the particle-fluid pair. Several authors have discussed the extension of R-Z to a wide range of particle characteristics and, until the present moment, there is good agreement in the literature about the estimation of n.

85

90

95

The parameter k represents the effect of the walls in the bed expansion. In theory, for narrower fluidized beds, the walls of the equipment should start to play a role in the bed expansion, while for larger equipment, the wall effect should be negligible, that is, k should be equal to 1. Nonetheless, the use of k and its dependence on the characteristics of the bed are still a divergence in the literature.

Richardson & Zaki [14] and Khan & Richardson [15], for example, proposed different correlations to calculate k as a function of the ratio between the equipment diameter and particle size (d_p/D) . In contrast, several authors achieved good agreement between the experimental and estimated bed porosities neglecting the wall effects, that is, assuming k = 1. Miura *et al.* [19], for example, have shown that, although the wall effects were not considered in their work,

the proposed correlations for the bed voidage obtained for Newtonian and non-Newtonian liquid-solid fluidized beds were not affected by this simplification. Moreover, Kramer *et al.* [20] found that wall effects can be neglected in case $Re_{t,\infty}>1$ -10. Still, Tang *et al.* [21] have shown that, when the particle size distribution is wide, the wall effect can decrease or increase the value of n depending on the particle size distribution. They observed, however, that the wall effect becomes more significant with decreasing bed diameter.

100

105

110

115

120

Alternatively, other authors, such as Rapagnà et al. [22] and Epstein [8], proposed other correlations for k as a function of the terminal settling Reynolds number $(Re_{t,\infty})$ instead of d_p/D .

According to Epstein [8], k can be estimated for a wide range of particles characteristics using the equation proposed by Khan & Richardson [15]:

$$k = 1 - 1.15 \left(\frac{d_p}{D}\right)^{0.6} \tag{3}$$

Lopes *et al.* [23], for example, obtained good agreement between prediction and experiments using the extended version R-Z by estimating k with Equation (3. Despite that, taking or not the wall effects into account, *i.e.*, the use of a calculated k in the R-Z equation and how to calculate it is still under debate.

Although the R-Z equation is widely used to estimate the bed expansion of liquid-solid fluidized beds, there is no consensus on what is the best way to estimate its parameters. Most of the studies found in the literature use very restrictive conditions to validate their correlations, hampering their applicability. Additionally, very few popular alternatives to R-Z were proposed so far, and most of them are direct correlations that take only the macro scale into account.

Aiming to fill these gaps, the present work investigates the extent of R-Z to 7 particles with a wide range of physical properties $(d_p, Ar, Re_{t,\infty})$. All particles are fluidized in water

using several different superficial velocities. The objective is to find the possible limitations of R-Z, using the convenient correlations for k and n proposed by Khan & Richardson. Since most details regarding the fluid-particle interactions at a meso scale are considered by drag correlations, an alternative to the bed porosity estimation using the correlations proposed by Di Felice [24], Beetstra *et al.* [25], and Rong *et al.* [26] is provided. To do this, the absolute difference between the Drag force calculated by the force balance for a single particle and the one estimated by each of the correlations was minimized to find the bed expansion, as explained further. Additionally, to assess the extent of the method, it was applied and compared to experimental data by Lopes *et al.* [23].

2. MATERIALS AND METHODS

To investigate the prediction of the bed expansion of liquid fluidized beds using R-Z and the proposed alternative method, experiments were performed using different particles. The materials and methods applied in the present work are described below.

2.1. Materials

125

130

135

140

145

The particles used in this work are divided into two big groups: heavy and light. Each group was characterized in terms of diameter, density, and terminal settling velocity. All heavy particles were used as acquired, while the light particles were synthesized. The heavy particles group comprises Acrylonitrile Butadiene Styrene (ABS, 5.95 mm diameter), porcelain (6.13 mm diameter), and two alumina (6.37 and 3.09 mm diameter) particles. The 3 light particles are all made of Barium Alginate (referred to as alginate particles).

The light particles were synthesized by dropping a 20 g/L sodium alginate (brand Fisher Chemical) solution into a 15 g/L barium chloride solution. When the sodium alginate droplets react with the barium chloride solution, the Barium Alginate particles are formed due to the gelification process. Titanium dioxide powder (mass ratio 25:2) was added to the sodium

alginate solution to increase the weight of the particles. Three different diameters of particles were obtained by changing the tip of the tubes and the flow rate of the sodium alginate solution. For a detailed description of the synthesis, the authors refer to Lopes *et al.* [23] and Melo *et al.* [27].

150

155

160

165

Densities of particles were measured by the pycnometry method, using a 25 mL pycnometer and distilled water as standard fluid. The diameter and circularity of the particles were measured using the OpenCV image processing library [28]. Pictures of the particles were taken maintaining the distance between them and the camera. Calibration of the software was done using the ABS particles as reference ($d_p = 5.95 \pm 0.01$ mm). The resulting diameters for each group of particles are equivalent to the superficial diameter of a set of 20 samples.

Terminal settling velocities of the particles were measured by tracking their falling trajectories inside a square base 20 cm wide water tank. The particle motion was recorded using a high-speed camera (correlation DSC-RX100 M, brand Sony) at 960 frames per second. The position tracking was done with the Tracker open-source image processing tool [29]. The terminal settling velocity corresponds to the average of ten particle launches. The average diameter, density, terminal settling velocity (± their respective standard deviations), and terminal Reynolds number of each particle are shown in Table 1. Images of the particles are also presented in Figure 1.

Table 1 – Properties of particles.

Particle	Density ρ_p	Diameter d_p	Terminal settling	Terminal Reynold
	(kg/m^3)	(mm)	velocity $U_{t,\infty}$	$Re_{t,\infty}$ (-)
			(cm/s)	
ABS	1823 ± 5	5.95 ± 0.07	39.45 ± 0.01	2840
Alumina (6.37 mm)	3573 ± 10	6.37 ± 0.21	71.12 ± 0.03	5485

Alumina (3.09 mm)	3586 ± 10	3.09 ± 0.16	48.02 ± 0.02	1795
Porcelain	2407 ± 3	6.13 ± 0.19	51.13 ± 0.02	3798
Alginate (4.76 mm)	1033 + 2	4.76 ± 0.27	6.04 ± 0.00	348
Alginate (3.48 mm)	1023 ± 2	3.48 ± 0.17	3.36 ± 0.00	142
Alginate (2.66 mm)	1029 ± 1	2.66 ± 0.10	3.03 ± 0.00	98

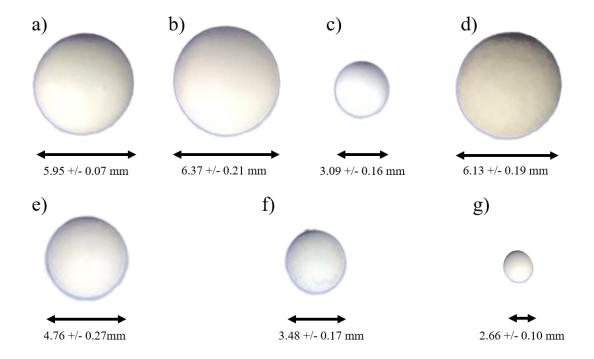


Figure 1. Images of the particles, being a) ABS, b) Alumina (6.37 mm), c) Alumina (3.09 mm), d) Porcelain, e) Alginate (4.76 mm), f) Alginate (3.48 mm), and g) Alginate (2.66 mm).

175

All experiments were carried out on the same fluidized bed setup, presented in Figure 1. The experimental setup, Figure 2a, comprises a liquid reservoir, a distributor, and the 10 cm diameter (D = 10 cm) vertical tube made of acrylic. A 1/2 Horsepower (HP) centrifugal pump pumps the liquid from the reservoir to the distributor. Below the distributor, there is a 10 cm height flow homogenizing portion full of packed glass beads. The particles are fluidized right

above the distributor, and the fluid flows throughout the 1 m height columns and back to the reservoir behind it.

180

185

190

Two different Arduino-based Hall effect sensors are used to measure the inlet flow rate of the fluid. For the experiments with the heavy particles, the YF-G1 (2-100 L/min) was used, while the YF-S201 (1-30 L/min) was applied for the light ones. The inlet flow rate was controlled by an inlet and a bypass valve. Before each experiment, the inlet flow rate was set to the given values, and the sensor registered both the time average and standard deviation of the measurements.

Additionally, the fluid temperature was monitored using a Negative Temperature Coefficient sensor (NTC). The average temperature in the experiments is 30 °C. This value was used to find the viscosity (μ) and density (ρ) of the fluid. The same characteristics of the liquid were used in the entire data.

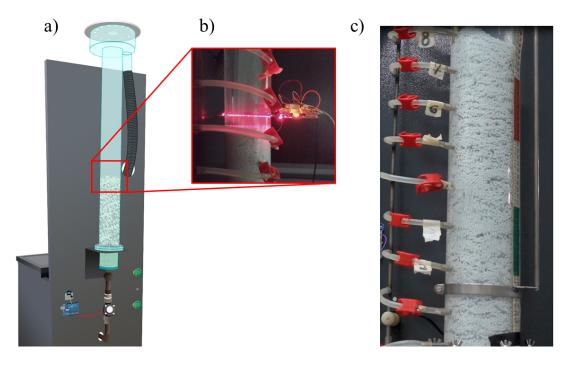


Figure 2. Schematic representation of a) the experimental setup, b) the laser apparatus, and c) the fluidization experiment.

2.2. Measurement of the bed expansion

At each replicate, a known mass of particles (M_p) was introduced into the column, and fluidization was established at a given liquid flow rate. The mass of particles, inlet flow rate range and the superficial Reynolds number $(Re = \rho UD/\mu)$ used in the fluidization experiments are shown in Table 2.

205

200

Bed heights were measured using the apparatus shown in Figure 2b. It comprises a 5V laser diode and a Light Dependent Resistor light sensor (LDR), pointed to each other at opposite sides of the equipment. Both the beam source and sensor are fixed to a small platform, which can be moved along the height of the equipment. The sensor measures the received light intensity and sends a proportional electric signal to an Arduino microcontroller, called analogic signal. Once the microcontroller is turned on, it starts registering the analogic signal. After 15 seconds of measurement, the microcontroller calculates an average among the registered values. In this work, this average value is referred to as laser (or beam) intensity.

Table 2 – Experimental conditions.

Particle	Total Mass	Number of	Liquid flow rate	Reynolds number Re
	M_p (kg)	liquid flow rates	range (l/min)	range (-)
ABS	2.0	11	25 - 75	6221 - 18664
Alumina (6.37 mm)	4.0	8	40 - 75	9954 - 18664
Alumina (3.09 mm)	4.0	8	40 - 75	9954 - 18664
Porcelain	2.7	11	25 - 75	6221 - 18664
Alginate (4.76 mm)	1.0	8	2 - 7	498 - 1742
Alginate (3.48 mm)	1.1	7	2 - 5	498 - 1244
Alginate (2.66 mm)	1.0	7	2 - 5	498 - 1244

The calibration of the sensor is done with the column full of water and with the particles in it. Before the experiments, the platform is positioned above the bed of particles so that the laser beam reaches the sensor without interruptions (as depicted in Figure 2b). This returns a high beam intensity to the microcontroller, which is the intensity in absence of particles. After this value is registered, the platform is positioned in the middle of the bed of particles. Because the particles are opaque, the light from the laser does not reach the sensor and the measured beam intensity is low. The average between both the high and low values is considered the threshold value. This value is used to identify the bed height.

215

220

During the fluidization experiments, the height of the laser was increased until the measured beam intensity was within 10% of the threshold value. This defined the height of the bed (H). This measurement method was highly reproducible, presenting a maximum standard deviation of 2% of the average. With the bed height H, the bed porosity (ε) was calculated using Equation (4:

$$\varepsilon = 1 - \frac{M_p/\rho_p}{\pi D^2 H} \tag{4}$$

The procedures adopted, the parameters measured, and the techniques used in the present work is summarized in the workflow presented in Figure 3.

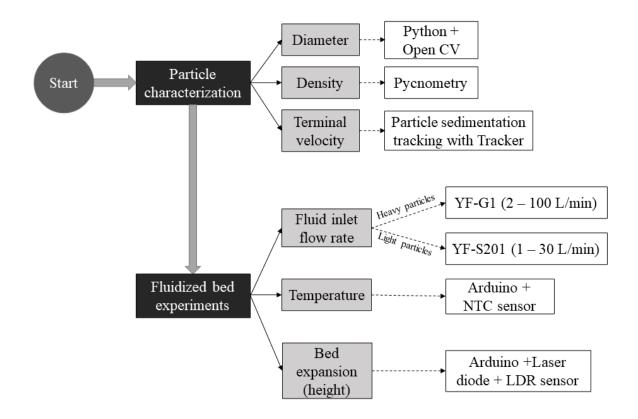


Figure 3. Workflow of the experimental procedure.

2.3. Bed expansion estimation

230

240

Expansion of the bed was estimated for all experimental conditions by two different methods. These values were further compared to the bed expansions obtained experimentally.

2.3.1. Richardson-Zaki (R-Z).

R-Z (Equation (1) was used to estimate the bed expansion given the superficial velocity of the fluid U and the experimental terminal settling velocity of the particles $U_{t,\infty}$. In this equation, the values of k and n were determined by the correlations proposed by Khan & Richardson [15] (Equations 2 and 3). Since some approaches to this equation neglect the parameter k, the expansion was also estimated for k = 1.

2.3.2. Drag Correlations

An alternative to the traditional R-Z was applied in the present work using drag correlations in the literature. Since the drag force acting over a single particle with volume V_p is

245

250

$$F_{D0} = V_p (\rho_p - \rho) g \tag{5}$$

and since the average drag force F_D can be estimated as a function of ε and Re_p using drag correlations in the literature, ε can be numerically found by minimizing $|F_D - F_{D0}|$. In the present work, this procedure was tested for the drag correlations proposed by Di Felice [24], Beetstra *et al.* [25] and Rong *et al.* [26] (referred to as Di Felice, Beetstra and Rong). Both Di Felice and Rong correlations follow a more traditional approach to the drag, which considers that, for a single particle inside the bed

$$F_D = \frac{1}{8} \rho U^2 C_D \pi d_p^2 G(\varepsilon, Re) \tag{6}$$

where C_D is the drag coefficient. According to Dallavalle [30],

$$C_D = \left(0.63 + \frac{4.8}{Re^{0.5}}\right)^2 \tag{7}$$

In Equation (7, $G(\varepsilon, Re) = \varepsilon^{-\beta}$. Di Felice and Rong proposed different correlations to calculate β , respectively written as

260

$$\beta = 3.7 - 0.65 \left[-\frac{(1.5 - logRe)^2}{2} \right]$$
 (8)

$$\beta = 2.65(\varepsilon + 1) - (5.3 - 3.5\varepsilon)\varepsilon^{2} \left[-\frac{(1.5 - logRe)^{2}}{2} \right]$$
 (9)

As a counterpart, Beetstra follows an alternative approach, proposing the following correlation.

$$F_{D} = 3\pi d_{p} U \left[\frac{10(1-\varepsilon)}{\varepsilon^{2}} + \varepsilon^{2} (1 + 1.5(1-\varepsilon)^{0.5}) + \frac{0.413Re}{24\varepsilon^{2}} \left(\frac{\varepsilon^{-1} + 3\varepsilon(1-\varepsilon) + 8.4Re^{-0.343}}{1 + 10^{3(1-\varepsilon)}Re^{-(1+4(1-\varepsilon))/2}} \right) \right]$$
(10)

In the present work, these 3 drag correlations are applied to find ε such that $|F_D - F_{D0}| < 10^{-10}$.

270 3. RESULTS AND DISCUSSION

275

280

The precise description of the fluidized bed expansion through simple equations is crucial to designing, maintaining, and optimizing LSFBs. For instance, the digestion of the biomass in wastewater and the yield of biogas production in LSFB bioreactors are directly related to the liquid fraction at the bed region. Overpredicting the bed expansion can lead to low conversions and problems related to controlling the biofilm thickness, while the underestimation of this parameter will lead to the washout of the particles. The bed porosity is directly related to velocity control. Using the described methodology, the bed porosity as a function of the inlet velocity was measured and estimated. The results for each particle are presented in Figure 4.

3.1. Bed expansion estimation using R-Z

Figure 2 presents the bed expansion as a function of the dimensionless superficial velocity $U/U_{t,\infty}$. The logarithmic scale highlights the linear trend amongst the experimental data. The errorbars correspond to one standard deviation. As shown in Figure 4, the standard deviation was very small, highlighting the reproducibility of the experiments. The highest standard

deviation among the experiments was found for the Alginate (2.66 mm) particles in the experiments with the lowest inlet flow rate (0.008644 m/s), corresponding to 1.89% of the average measured porosity.

285

290

According to Epstein [8], the correlation should be accurate for particles with $0.01 < Re_{t,\infty} < 7000$ and $0.001 < d_p/D < 0.2$; that is, all particles in this work. Nonetheless, as shown by the coefficient of determination (R^2) , the R-Z using Khan & Richardson [15] k presented better fitting for the higher diameter particles (Figure 4a, b, and d, respectively). This suggests that the k may be less sensitive to d_p/D than indicated by Khan & Richardson [15], which could justify the better fitting between the experiments and R-Z with k=1 for small and intermediary alginate beads (Figure 4f and g, respectively).

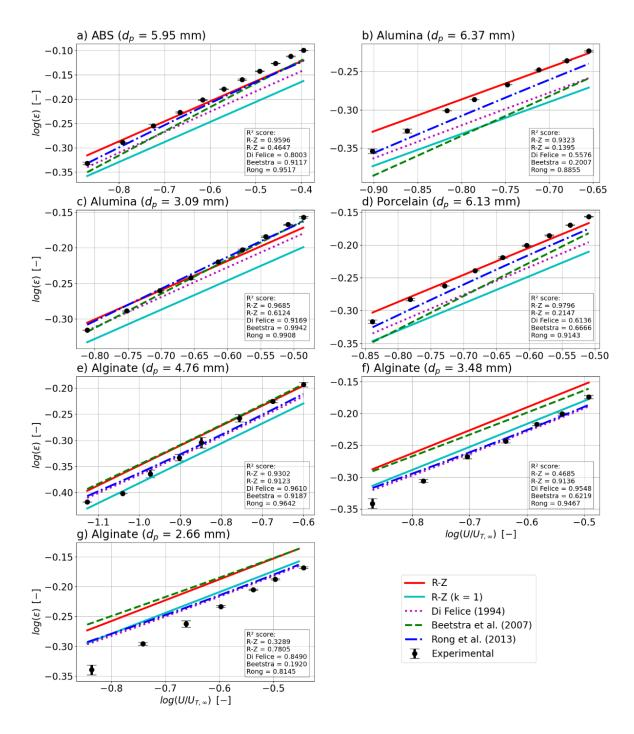


Figure 4. Bed voidage vs. $U/U_{t,\infty}$ in logarithmic scale +/- standard deviation for a) ABS, b) Alumina (6.37 mm), c) Alumina (3.09 mm), d) Porcelain, e) Alginate (4.76 mm) Alginate (3.48 mm), and g) Alginate (2.66 mm) particles.

300

However, comparing the R^2 for R-Z in Figure 4c and f it is noted that R-Z fitted better to the smaller alumina (3.09 mm) than to the slightly larger alginate particle (3.48 mm). Since the density ratio between the alumina and alginate is 3 to 1, this shows that the value of k is also dependent on the pair fluid-particle characteristics, *i.e.*, Ar or $Re_{t,\infty}$, for instance. Following the

principle of Fidleris & Withmore [31] for a single particle, Dharmarajah & Cleasby [32] showed that the wall effect is not negligible for pilot-scale experiments, mainly if scale-up is intended. The authors highlight the importance of $Re_{t,\infty}$ together with d_p/D to the wall effect. More recently, Akgiray & Soyer [1] highlighted the same feature based on new experiments and data in the literature. The correlations proposed in both works are detached from the traditional R-Z correlation and are currently not as prominent.

305

310

315

320

325

By contrast, Rapagnà et~al.~ [22] and Epstein [8] proposed two correlations to estimate k based exclusively on $Re_{t,\infty}$ with good fitting to the experimental data, but with limited ranges of $Re_{t,\infty}$. According to Epstein [8], Equation (2 can be used for a wide range of $Re_{t,\infty}$. The author recommends the use of Rapagnà et~al.~ [22] correlation when it gives a lower value than Equation (2 for particles presenting $100 < Re_{t,\infty} < 1000$. The same for the equation proposed by the author for $35 < Re_{t,\infty} < 100$, whereas this was not the case with the particles in this work.

To find an experimental value for k, a linear regression was applied to the experimental data on a logarithmic scale. In Figure 5, the values of k obtained from the regression and calculated using the Khan and Richardson correlation are shown.

The approach to R-Z proposed by Epstein [8] was recently applied by Lopes $et\ al.$ [23] to predict the expansion of a fluidized bed of particles like the one used in the present work. According to the authors, the lack of agreement between the experimental and the predictions using the k of Khan & Richardson could be explained by the mechanical properties of the particles, i.e., the soft and light particles tend to agglomerate due to their low effective coefficient of restitution and stokes number, which would increase the drag acting over the particles. The results in the present work bring up a new hypothesis for such deviations, since, as can be seen in Figure 5, k was also higher than predicted for the rigid porcelain, ABS, and larger alumina particles.

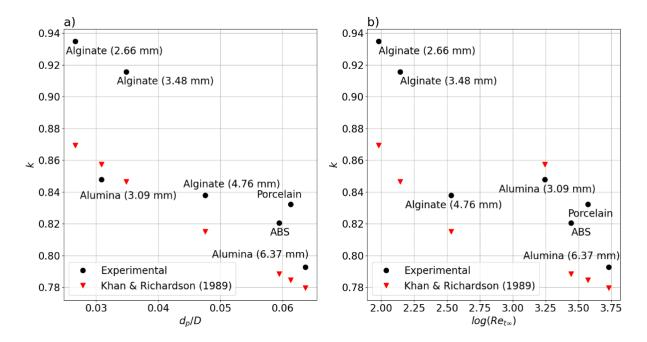


Figure 5. k as a function of a) d_n/D , and b) $ln(Re_{t,\infty})$.

335

340

As can be noted from Figure 5, the Khan & Richardson correlation is more likely to accurately predict k for higher values of $Re_{t\infty}$. On the other hand, the highest relative deviation between the experimental and predicted k is 6.99% for the smaller alginate particle. It shows that the estimation of the bed porosity using R-Z is notably sensitive to the parameter estimation, especially considering lower values of d_p/D . This lack of robustness makes the pilot-scale experiments less likely to represent full-scale equipment and the use of R-Z correlation may lead to incorrect prediction of the bed expansion.

3.2. Bed expansion estimation using drag correlations

R-Z is particularly powerful with k=1 to represent the drag acting over the particles at given porosities. As discussed in the Introduction, several authors choose to neglect the effect of k = 1 for various applications, either by justifying that the wall effect is negligible for full-scale equipment or to reduce the number of parameters. In all works, good fittings are achieved by the correlations proposed to n. For instance, Di Felice [24], Beetstra *et al.* [25], Rong *et al.* [26], and Mazzei & Lettieri [33] developed drag correlations by decomposing forces and

isolating the effect of the drag from the summation of particle-fluid forces (buoyancy, pressure gradient, shear stress, and others). More recently, with the advance of computational power, these and other correlations based on the same approach are applied in numerical simulations of multiphase systems (such as cyclones, fluidized beds, and others), presenting good agreement with empirical data.

345

350

355

360

365

In the present work, the numerical approach was simplified to determine the expansion of the bed based on consolidated drag correlations. In this approach, ε was estimated by minimizing the objective function $|F_D - F_{D0}|$, that is, the absolute difference between Equation (5 and the drag correlations. The results of this approach for the Di Felice [24], Beetstra *et al.* [25], Rong *et al.* [26] drag correlations (called from this point Di Felice, Beetstra, and Rong correlations, respectively) are presented in Figure 4. A better comparison can be done using the R^2 of the adjustments, which is presented in Figure 6.

Di Felice and Beetstra correlations were not consistent in the agreement between experimental and predicted results. In the case of Di Felice, the lack of fitting was found mainly for the porcelain and larger alumina particles ($R^2 = 0.56$ and 0.61, respectively), that is, the larger particles amongst those tested. Beetstra correlation was the most inconsistent among the correlations, presenting good fitting only for the ABS, smaller alumina, and larger alginate particles. This shows that the correlations, using this minimization approach, can be more sensitive to the characteristics of the multiphase system (d_p/D , Ar, $Re_{t,\infty}$).

On the other hand, the minimization approach using the Rong drag correlation presents higher potential since its R^2 is between 0.81 (smaller alginate, Figure 4g) and 0.99 (smaller alumina, Figure 4c). For 4 among the 7 particles, this approach presented better fitting than the R-Z using the correlations for n and k proposed by Khan & Richardson [15]. The results for the larger alumina particles, in which R-Z presented a higher R^2 than the Rong correlation, the difference was around 5%. Alternatively, for the intermediary and smaller alginate

particles, the Rong correlation showed R^2 around two times higher than R-Z with k.

370

375

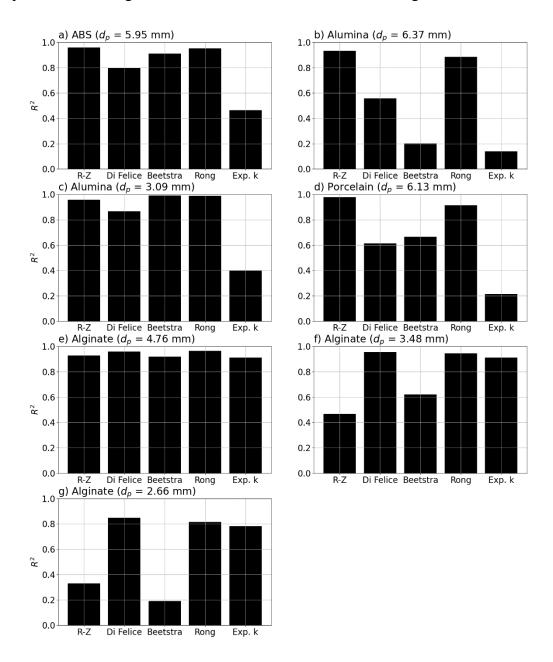


Figure 6. R^2 of the different methods of bed expansion estimation for a) ABS, b) Alumina (6.37 mm), c) Alumina (3.09 mm), d) Porcelain, e) Alginate (4.76 mf) Alginate (3.48 mm), and g) Alginate (2.66 mm) particles.

The difference between Di Felice and Rong correlations is attributed to the way the β is calculated for each correlation. Di Felice and Rong share the same formulation for F_D , with C_{D0} calculated by the well-established Dallavalle [33] correlation. In Di Felice correlation, β is not a function of ε , which was shown by many authors, including Beetstra *et al.* [28] and Rong *et al.* [29], to lead to significant uncertainties on the average drag estimation. Rong correlation

includes the effect of the porosity on β by fitting data obtained by Lattice-Boltzmann simulations. In verification with experimental results, Rong reduced the overall deviation by half (around 15%) compared to the other correlations tested in this work (25 to 30%). In the case of Beetstra correlation, besides accounting for both the Re_p and ε , the completely different formulation for C_{D0} , which is different from the one of Dallavalle, may be the reason for the additional inaccuracies.

380

385

390

395

400

It is important to note that the Rong drag correlation does not take the wall effect into account. Since it has better agreement than R-Z, Rong correlations is more capable of capturing the dependence of the expansion with the fluid-particle pair characteristics (i.e., Ar or $Re_{t,\infty}$) than the Khan & Richardson correlation for k. This difference between Rong and R-Z highlights the dependence between k and the fluid-particle interactions beyond wall effects. Most likely, both d_p/D and Ar (or $Re_{t,\infty}$) should be combined to find better correlations for k, as shown by Dharmarajah & Cleasby [32] and Akgiray & Soyer [1]. Since such a correlation is not yet established and the Rong correlation has been tested for a wide range of regimes, the fast and computational cheap minimization approach using the Rong correlation is a good alternative based on the present results.

3.3. Extrapolation of the proposed method

To assess its extent, the proposed numerical method was applied and compared to results obtained by Lopes *et al.* [23]. The work was chosen due to the similarity between the experimental setups. In their study, particles with different characteristics (Table 2) were fluidized by water in a 19-mm-diameter column (almost twice the diameter of the column used in the present work). The liquid fludized bed expansion was also investigated for a variety of particles and regimes, with inlet Reynolds numbers between 2940 and 11779.

Table 3 – Experimental conditions.

Particle	Density ρ_p	Diameter d_p	Terminal settling	Terminal Reynold
	(kg/m^3)	(mm)	velocity $U_{t,\infty}$ (cm/s)	$Re_{t,\infty}$ (-)
Glass	2500 ± 10	1.85 ± 0.11	25.7 ± 1.8	357
ABS (uncoated)	1965 ± 2	5.87 ± 0.01	38.4 ± 2.8	1859
ABS (uniformly coated)	1913 ± 10	5.96 ± 0.01	38.7 ± 1.6	1898
ABS (non-uniformly coated)	1919 ± 12	5.94 ± 0.01	36.3 ± 2.0	1777
Alginate (Calcium)	1228 ± 8	4.88 ± 0.32	14.0 ± 1.2	647
Alginate (Cobalt)	1110 ± 5	5.83 ± 0.45	12.1 ± 1.2	619
Starch Pearls	1080 ± 6	12.18 ± 0.56	14.3 ± 0.6	1673

For this comparison, the Rong correlation was chosen for presenting the best fitting with the experimental data of this work. Figure 7 shows the coefficient of correlation R^2 of the adjustment between the experimental results of Lopes *et al.* [23] and estimations using the proposed approach and R-Z (also extracted from Lopes *et al.* [23]).

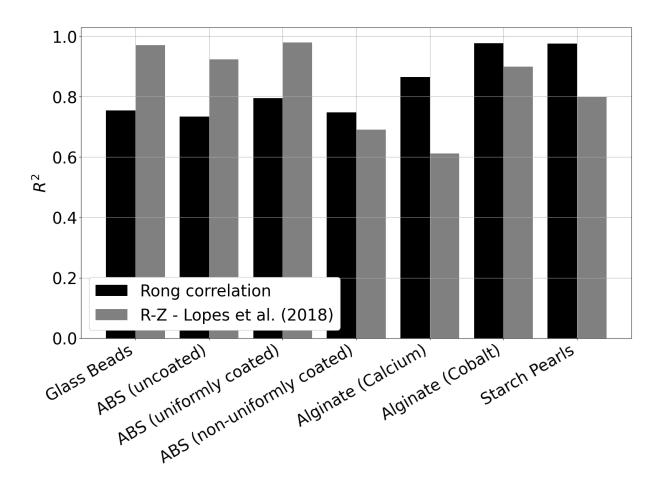


Figure 7. R^2 of the fitting between experiments by Lopes *et al.* [23] and estimations using R-Z and Rong drag correlation.

420

The average R^2 for R-Z and the numerical approach using Rong correlation were 0.84. Although R-Z was better to represent the data obtained for the glass beads and some of the ABS particles, the proposed approach presented better results for most of the particles (4 out of the 7) investigated. Additionally, the lowest R^2 found using the proposed drag correlation approach was 0.73 (uncoated ABS), while for R-Z, it was 0.61 (Alginate made with calcium chloride). These results highlight not only the precision, but also the scalability of the method, given that the diameter of the equipment (0.1905 m) is almost two times the one described in the present work.

4. **CONCLUSION**

425

430

435

440

445

The results of bed expansion estimated from the Richardson-Zaki equation were compared to experimental data obtained for several inlet velocities, using 7 particles with significantly different diameters, densities, Archimedes numbers, and terminal velocities. The aim was to determine if R-Z can predict the bed expansion for a wide variety of particles and flow regimes. Since the literature presents good agreement about the R-Z index n, the present work focuses the discussion on the parameter k. It was shown that the use of the parameter k is strongly case dependent, with no specific criterium, and still needs further investigation.

Apart from that, an alternative approach to predict bed expansion was tested, presenting promising results. The minimization approach using the drag correlations showed better agreement than R-Z for 4 out of the 7 particles. Among the drag correlations, the one proposed by Rong showed the best fitting, being consistently accurate for the wide range of particles considered in the present work. This approach was also validated against the experimental data by Lopes *et al.* [23].

The main drawback of the proposed method is that the force balance is applied to the entire bed, without taking the particles distribution into account. This means that it will be more precise the more uniform the bed is, which is true for most monodispersed liquid fluidized beds. Additionally, the proposed method is iteractive, meaning that it is not as directly applicable as R-Z. Nonetheless, the use of fully black box correlations to calculate the parameters n and k leads to unpredictability, which is not the case in the proposed method.

It is important to note that none of the drag correlations take the wall effects into account. Considering that the Rong correlation presented better accuracy amongst the results, the correction due to the wall effects using the parameter k may not be the key to the prediction of the bed expansion in pilot scale experiments or even the right correction for the scale-up. This fact highlights the need for more robust methods to predict bed expansion, and the minimization

approach presented in this paper can be a good alternative for this due to its negligible computational cost and high accuracy. Additionally, since the method is based on the force balance applied to the bed of particles and it was validated for a wide range of regimes, this approach can be easily and reliably applied to pairs other than particle-water, especially in the broad investigated range of Reynolds and Archimedes numbers. The proposed method using the Rong drag correlation improves the predictability of the liquid fluidized bed operating conditions, consequently spreading the fluidization technologies to industrial applications in which they have a high potential such as wastewater treatment and biogas production plants.

ACKNOWLEDGMENT

Thanks are due to São Paulo Research Foundation (FAPESP, grant #2019/19173-9, grant #2020/14567-6, and grant #2019/25146-4); the Funding Authority for Studies and Projects of the Ministry of Science, Technology and Innovation (FINEP/MCTI) by means of the Program of Human Resources of the Brazilian National Petroleum Agency (PRH-ANP/MCTI); and the Brazilian National Council for Scientific and Technological Development (CNPq, process number 408618/2018-3) for financial support. The authors also thank Federal University of São Carlos (UFSCar) for the infrastructure and Polytechnique Montréal for the technical support. This study was financed in part by the Coordenação de Aperfeiçoamento de Pessoal de Nível Superior – Brasil (CAPES) – Finance Code 001. Bruno Blais acknowledges the financial support from the Natural Sciences and Engineering Research Council of Canada (NSERC) through the RGPIN-2020-04510 Discovery grant.

470

450

455

460

465

DECLARATIONS

Funding

This study was financed in part by the Coordenação de Aperfeiçoamento de Pessoal de Nível Superior - Brasil (CAPES) - Finance Code 001; São Paulo Research Foundation (FAPESP, grant #2019/19173-9, grant #2020/14567-6, and grant #2019/25146-4); Funding Authority for Studies and Projects of the Ministry of Science, Technology and Innovation (FINEP/MCTI) by means of the Program of Human Resources of the Brazilian National Petroleum Agency (PRH-ANP/MCTI); and the Brazilian National Council for Scientific and Technological Development (CNPq, process number 408618/2018-3). Bruno Blais acknowledges the financial support from the Natural Sciences and Engineering Research Council of Canada (NSERC) through the RGPIN-2020-04510 Discovery grant.

Conflict of interest/competing interests

The authors declare that they have no competing interests.

Availability of data and material

Not applicable.

Code availability

Not applicable.

Authors' contributions

All authors contributed to the manuscript's conception. The experimental steps, such as material preparation, were carried out by Victor Oliveira Ferreira, Daniel Silva Junior, and Karla Raphaela Braga de Melo. All steps were supervised by Gabriela Cantarelli Lopes, the project coordinator. Bruno Blais contributed to the definition of the project and helped in discussing the results. All authors commented and contributed to previous versions of the article. All authors read and approved the final manuscript.

495

490

475

480

NOMENCLATURE

Archimedes number (-)
drag coefficient
diameter of the column (cm)
diameter of the particles (mm)
drag force over a particle inside the bad
drag force acting over a single particle
gravity acceleration (m/s²)
bed height (m)
Richardson-Zaki wall effect parameter (-)
total mass of particles in the experiments (kg)
Richardson-Zaki index (-)
Reynolds number of the flow (-)
Reynolds number of the particle at terminal settling velocity (-)
inlet (surficial) fluid velocity (m/s)
terminal settling velocity of the particle (cm/s)
drag index
voidage (porosity) of the bed
dynamic viscosity (Pa.s)
fluid density (kg/m³)
particle density (kg/m³)

REFERENCES

- [1] O. Akgiray and E. Soyer, "An evaluation of expansion equations for fluidized solid–liquid systems," *Journal of Water Supply: Research and Technology-Aqua*, vol. 55, p. 517–526, November 2006.
- [2] R. Aldaco, A. Garea and A. Irabien, "Modeling of particle growth: Application to water treatment in a fluidized bed reactor," *Chemical Engineering Journal*, vol. 134, p. 66–71, November 2007.
- [3] A. K. Mukherjee, B. K. Mishra and R. V. Kumar, "Application of liquid/solid fluidization technique in beneficiation of fines," *International Journal of Mineral Processing*, vol. 92, p. 67–73, July 2009.
- [4] T. R. Dias, W. R. Melchert, M. Y. Kamogawa, F. R. P. Rocha and E. A. G. Zagatto, "Fluidized particles in flow analysis: potentialities, limitations and applications," *Talanta*, vol. 184, p. 325–331, July 2018.
- [5] M. M. Bello, A. A. A. Raman and M. Purushothaman, "Applications of fluidized bed reactors in wastewater treatment A review of the major design and operational parameters," *Journal of Cleaner Production*, vol. 141, p. 1492–1514, January 2017.
- [6] S. D. Naghib, V. Pandolfi, U. Pereira, R. Girimonte, E. Curcio, F. P. D. Maio, C. Legallais and A. D. Renzo, "Expansion properties of alginate beads as cell carrier in the fluidized bed bioartificial liver," *Powder Technology*, vol. 316, p. 711–717, July 2017.
- [7] N. Epstein, "Applications of Liquid-Solid Fluidization," *International Journal of Chemical Reactor Engineering*, vol. 1, November 2002.

- [8] N. Epstein, "Liquid-solids fluidization," W. Yang, Ed., Marcel Dekker, New York, NY, USA, 2003.
- [9] N. S. Jamali, J. M. Jahim, W. N. R. W. Isahak and P. M. Abdul, "Particle size variations of activated carbon on biofilm formation in thermophilic biohydrogen production from palm oil mill effluent," *Energy Conversion and Management*, vol. 141, p. 354–366, June 2017.
- [10] A. Elreedy, A. Tawfik, A. Enitan, S. Kumari and F. Bux, "Pathways of 3-biofules (hydrogen, ethanol and methane) production from petrochemical industry wastewater via anaerobic packed bed baffled reactor inoculated with mixed culture bacteria," *Energy Conversion and Management*, vol. 122, p. 119–130, August 2016.
- [11] S. D. Fraia, N. Massarotti and L. Vanoli, "A novel energy assessment of urban wastewater treatment plants," *Energy Conversion and Management*, vol. 163, p. 304–313, May 2018.
- [12] H. Nadais, M. Barbosa, I. Capela, L. Arroja, C. G. Ramos, A. Grilo, S. A. Sousa and J. H. Leitão, "Enhancing wastewater degradation and biogas production by intermittent operation of UASB reactors," *Energy*, vol. 36, p. 2164–2168, April 2011.
- [13] P. Metolina and G. C. Lopes, "Numerical analysis of liquid-solid flow in tapered and cylindrical fluidized beds for wastewater treatment and biogas production," *Energy Conversion and Management*, vol. 187, p. 447–458, May 2019.
- [14] J. F. Richardson and W. N. Zaki, "Sedimentation and fluidisation: Part I," *Chemical Engineering Research and Design*, vol. 75, p. S82–S100, December 1997.

- [15] A. R. Khan and J. F. Richardson, "Fluid-Particle Interactions and Flow Characteristics of Fluidized Beds and Settling Suspensions of Spherical Particles," *Chemical Engineering Communications*, vol. 78, p. 111–130, April 1989.
- [16] G. B. Wallis, One-dimensional two-phase flow, Courier Dover Publications, 2020.
- [17] J. Garside and M. R. Al-Dibouni, "Velocity-Voidage Relationships for Fluidization and Sedimentation in Solid-Liquid Systems," *Industrial & Engineering Chemistry Process Design and Development*, vol. 16, p. 206–214, April 1977.
- [18] P. N. Rowe, "A convenient empirical equation for estimation of the Richardson-Zaki exponent," *Chemical Engineering Science*, vol. 42, p. 2795–2796, 1987.
- [19] H. Miura, T. Takahashi, J. Ichikawa and Y. Kawase, "Bed expansion in liquid-solid two-phase fluidized beds with Newtonian and non-Newtonian fluids over the wide range of Reynolds numbers," *Powder Technology*, vol. 117, p. 239–246, June 2001.
- [20] O. J. I. Kramer, P. J. de Moel, E. T. Baars, W. H. van Vugt, J. T. Padding and J. P. van der Hoek, "Improvement of the Richardson-Zaki liquid-solid fluidisation model on the basis of hydraulics," *Powder Technology*, vol. 343, p. 465–478, February 2019.
- [21] C. Tang, M. Liu and Y. Li, "Experimental investigation of hydrodynamics of liquid–solid mini-fluidized beds," *Particuology*, vol. 27, p. 102–109, August 2016.
- [22] S. Rapagnà, R. Di Felice, L. G. Gibilaro and P. U. Foslcolo, "Steady-State Expansion Characteristics of Monosized," *Chemical Engineering Communications*, vol. 79, p. 131–140, May 1989.

- [23] G. C. Lopes, X. Bi, N. Epstein, S. A. Baldwin and J. R. Grace, "Hydrodynamic characteristics of particles with different roughness and deformability in a liquid fluidized bed," *Chemical Engineering Science*, vol. 185, p. 50–63, August 2018.
- [24] R. Di Felice, "The voidage function for fluid-particle interaction systems," *International Journal of Multiphase Flow*, vol. 20, p. 153–159, February 1994.
- [25] R. Beetstra, M. A. van der Hoef and J. A. M. Kuipers, "Drag force of intermediate Reynolds number flow past mono- and bidisperse arrays of spheres," *AIChE Journal*, vol. 53, p. 489–501, 2007.
- [26] L. W. Rong, K. J. Dong and A. B. Yu, "Lattice-Boltzmann simulation of fluid flow through packed beds of uniform spheres: Effect of porosity," *Chemical Engineering Science*, vol. 99, p. 44–58, August 2013.
- [27] K. R. B. Melo, T. F. de Pádua and G. C. Lopes, "A coefficient of restitution model for particle–surface collision of particles with a wide range of mechanical characteristics," *Advanced Powder Technology*, vol. 32, p. 4723–4733, December 2021.
- [28] G. Bradski, "The OpenCV Library," Dr. Dobb's Journal of Software Tools, 2000.
- [29] Tracker Video Analysis and Modeling Tool, 2022.
- [30] J. M. Dalla Valle, Micromeritics: The Technology of Fine Particles, Pitman, 1948.
- [31] V. Fidleris and R. L. Whitmore, "Experimental determination of the wall effect for spheres falling axially in cylindrical vessels," *British journal of applied physics*, vol. 12, p. 490, 1961.

- [32] A. H. Dharmarajah and J. L. Cleasby, "Predicting the Expansion Behavior of Filter Media," *Journal American Water Works Association*, vol. 78, p. 66–76, December 1986.
- [33] L. Mazzei and P. Lettieri, "A drag force closure for uniformly dispersed fluidized suspensions," *Chemical Engineering Science*, vol. 62, p. 6129–6142, November 2007.